A new numeric technique for high-speed evaluation of power system frequency

P.J. Moore, PhD, CEng, MIEE
R.D. Carranza, MSc
A.T. Johns, DSc, CEng, FIEE

Indexing terms: Power system, Frequency measurement

Abstract: A new numeric technique for evaluating power system frequency from either a voltage or current signal is presented. The technique uses discrete time values of the input signal, taken at a fixed sampling rate, to provide an estimate of power system frequency accurate to within typically 0.001 Hz. The technique is shown to be capable of tracking frequency under dynamic power systems conditions and is immune to the effect of harmonics. It is further shown that the algorithm can be easily adapted to process three-phase signals such that the positive phase sequence component can be utilised thus increasing the reliability of the measurement under fault conditions.

List of symbols

$x(t)$ = continuous form of measured power system quantity (e.g. voltage or current)
$x'(t)$ = time derivative of $x(t)$
$x(n\Delta T)$ = discrete time form of measured power system quantity (e.g. voltage or current), usually abbreviated to $x(n)$
ΔT = sampling interval
f_s = sampling frequency, $f_s = 1/\Delta T$
f = apparent power system frequency
f_0 = nominal power system frequency
$H(k)$ = coefficients of finite impulse response filter (for $k = 0, \ldots, N-1$, $N = f_s/f_0$)
z = Z transform operator
Ω = normalised frequency, $\Omega = 2\pi f/f_s$

1 Introduction

Accurate monitoring of the frequency of a power system is essential to optimum operation. Variations in frequency from a nominal value can be, for example, indicative of unexpected system disturbances for which some corrective action must be taken. On a large, stiff power system, variations in frequency will usually be slow due to the large mechanical inertia of the system. However, on smaller systems, changes in frequency will be correspondingly faster. In either case, it is imperative to determine frequency deviations at the earliest stage.

The use of microprocessor technology has produced many benefits in the field of power system protection, monitoring and control. The ability of microprocessor-based devices to provide fast response to changing system conditions is well known and their use for measuring power system frequency is well established. Early work reported in this area [1, 2] suffered from excessively long frequency evaluation times although more recent work has seen a steady improvement. The simplest method of frequency evaluation involves timing signal zero crossings [3, 4] although this approach is still relatively slow since it requires a large amount of input data to detect small deviations. Adaptation of the sampling interval to ensure correct measurement using an algorithm based on the discrete Fourier transform is feasible [5] although it is prone to round off oscillations since the sampling interval cannot be infinitely varied. Most of these methods assume that the statistics of the power system are stationary, that is, do not vary with time. Alternatively, assumptions based on known power system statistics can be used [6]. Several authors have incorporated least mean squares estimation theory using both stationary models [7, 8] and adaptive estimation, where the frequency is tracked without any prior statistical knowledge [9, 10]. However, all such methods involve a compromise between the accuracy of the frequency measurement and the length of the observation period: accuracy decreases as the period becomes smaller.

The algorithm described herein is designed to provide the fastest estimate of power system frequency based upon analysis of approximately one cycle of a sampled power system waveform. To ensure high accuracy, the algorithm uses a relatively high sampling frequency (4 kHz) to give good numeric representation of the input signal. Unlike other methods, the algorithm does not rely on zero crossings or statistical knowledge of the power system. It does not require any special hardware other than that usually found within microprocessor based protection relay equipment, and it uses a fixed sampling frequency, thus avoiding the need for, and practical problems associated with, the use of sampling frequency variation means.

Paper 1360C (P11), received 8th February 1994

The authors are with the School of Electronic and Electrical Engineering, University of Bath, Bath, BA2 7AY, United Kingdom

The authors are grateful for the provision of facilities in the Power and Energy Systems Research Group at the University of Bath. The second author would like to thank CONACYT-Mexico for financial support.

2 Algorithm development

2.1 Basic principle

Let a continuous power system voltage or current be denoted by $x(t)$. Decomposing $x(t)$ into two components which are orthogonal in phase gives

$$x_{1(t)} = X \sin(2\pi ft + \phi) \tag{1}$$

and

$$x_2(t) = X \cos(2\pi ft + \phi) \tag{2}$$

where subscripts 1 and 2 denote the individual components, X is the magnitude and f is the frequency of the signal $x(t)$, and ϕ is an arbitrary phase shift.

Differentiating eqns. 1 and 2 with respect to time gives:

$$\frac{d[x_1(t)]}{dt} = 2\pi fX \cos(2\pi ft + \phi) = x'_1(t) \tag{3}$$

and

$$\frac{d[x_2(t)]}{dt} = -2\pi fX \sin(2\pi ft + \phi) = x'_2(t) \tag{4}$$

Eqns. 1 to 4 may be rearranged as

$$\begin{aligned} &x_2(t)x'_1(t) - x_1(t)x'_2(t) \\ &\quad = 2\pi fX^2 \cos^2(2\pi ft + \phi) + 2\pi fX^2 \sin^2(2\pi ft + \phi) \\ &\quad = 2\pi fX^2 \end{aligned} \tag{5}$$

which is seen to be directly proportional to the product of the frequency and the square of the amplitude. To remove the amplitude dependency, the following expression is used:

$$\begin{aligned} &x_1^2(t) + x_2^2(t) \\ &\quad = X^2 \cos^2(2\pi ft + \phi) + X^2 \sin^2(2\pi ft + \phi) \\ &\quad = X^2 \end{aligned} \tag{6}$$

Thus, combining eqns. 5 and 6 yields

$$f = \frac{x_2(t)x'_1(t) - x_1(t)x'_2(t)}{2\pi[x_1^2(t) + x_2^2(t)]} \tag{7}$$

Eqn. 7 is an analytic expression for the frequency of $x(t)$ derived from its two orthogonal components and their time derivatives.

2.2 Frequency calculation from discrete time signals

Eqn. 7 may be applied to discrete time signals by replacing $x(t)$ with $x(n\Delta T)$ where ΔT is the sampling period and $\Delta T = 1/f_s$ where f_s is the sampling frequency. For clarity, $x(n\Delta T)$ will be written simply as $x(n)$ from here on.

The discrete time signal $x(n)$ may be decomposed into two components, each orthogonal in phase, by the use of two finite impulse response (FIR) filters based upon sine and cosine impulse responses. This technique is actually identical to the discrete Fourier transform evaluated for the fundamental component. However, it is more convenient to consider the orthogonalisation being effected by two FIR filters. The coefficients of the FIR filters are evaluated as

$$H_s(k) = \sin\left(\frac{2\pi k}{N} + \frac{\pi}{N}\right) \tag{8}$$

and

$$H_c(k) = \cos\left(\frac{2\pi k}{N} + \frac{\pi}{N}\right) \tag{9}$$

where $k = 0, 1, 2, \ldots, N-1$, $N = f_s/f_0$, f_0 = nominal power system frequency.

Hence, the two orthogonal components of $x(n)$ may be evaluated by digital convolution as

$$x_1(n) = \sum_{k=0}^{N-1} x(n-k)H_s(k) \tag{10}$$

and

$$x_2(n) = \sum_{k=0}^{N-1} x(n-k)H_c(k) \tag{11}$$

To calculate the time derivative of the orthogonalised signals, piecewise linearity between the samples is assumed which allows the following backward difference equation to be used:

$$x'(n) = \frac{[x(n) - x(n-1)]}{\Delta T} \tag{12}$$

Eqn. 12 can be applied to both orthogonal components of $x(n)$. To retain accuracy of the derivative, it is advantageous to keep the time difference between the two elements of the right hand side of eqn. 12 as small as possible; the equation thus represents the minimum situation. However, a drawback to this approach lies in the fact that the derivative approximated is most representative of a point mid-way between the two samples of $x(n)$. Potential errors arising from this may be compensated for by substituting $x(n)$ with the arithmetic mean of $x(n)$ and $x(n-1)$. Hence the discrete time equivalent of eqn. 7 is given by

$$f \approx \frac{1}{2\pi} \frac{\left(\frac{x_2(n) + x_2(n-1)}{2}\right)x'_1(n) - \left(\frac{x_1(n) + x_1(n-1)}{2}\right)x'_2(n)}{\left(\frac{x_1(n) + x_1(n-1)}{2}\right)^2 + \left(\frac{x_2(n) + x_2(n-1)}{2}\right)^2} \tag{13}$$

which reduces to

$$f \approx \frac{1}{\pi T} \frac{(x_2(n) + x_2(n-1))x'_1(n) - (x_1(n) + x_1(n-1))x'_2(n)}{(x_1(n) + x_1(n-1))^2 + (x_2(n) + x_2(n-1))^2} \tag{14}$$

2.3 Errors due to discrete time representation

The discrete time representation of the input signal, and its subsequent processing, cause two significant sources of error when eqn. 14 is used to evaluate the apparent frequency of the input signal. The first, and most significant, arises due to the FIR filters having different magnitude gains at frequencies other than the nominal power system frequency. The second cause of error is introduced by the numerical computation of the derivative.

The FIR filters described by eqns. 8 to 11 are used to produce components of the input signal $x(n)$ which are orthogonal in phase. The phase characteristic of any FIR filter having an impulse response which is either symmetric or antisymmetric, is linear with frequency. The use of one FIR filter based on a cosine function (antisymmetric impulse response), and the other based on a sine function (symmetric impulse response), ensures that the filter outputs differ by 90° for all input signal frequencies. However, although the phase characteristics

of these filters perform ideally for the required function, the magnitude characteristics are far from perfect. Fig. 1*a* shows that the magnitude responses of the sine and cosine based FIR filters are not identical. Fig. 1*b* shows

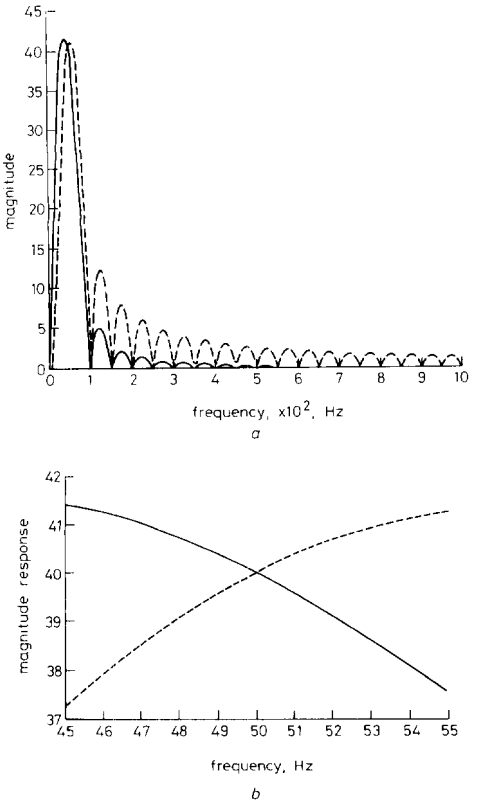

Fig. 1 *Frequency magnitude response for othogonal filters*
a Assuming f_s = 4 kHz, for clarity only 0–1 kHz range displayed
b Expanded view of *a* in the range 45–55 Hz
—— Sine filter
····· cosine filter

an expanded section of Fig. 1*a* in the region of 45–55 Hz from which it will be apparent that the magnitude gains of the filters are only equal at exactly the nominal power system frequency of, in this case, 50 Hz. This implies that the orthogonalised signals $x_1(n)$ and $x_2(n)$ have frequency dependent magnitude gains. Since eqn. 14 assumes the orthogonalised signal gains to be frequency independent, an error will be introduced if account is not taken of this effect.

It is shown in Appendix 7.1 that the magnitude gains of the sine and cosine filters are given by:

$$|H_s(f)| = \frac{2 \sin(\pi f_0/f_s) \sin(\pi N f/f_s) \cos(\pi f/f_s)}{\cos(2\pi f/f_s) - \cos(2\pi f_0/f_s)} \quad (15)$$

and

$$|H_c(f)| = \frac{2 \cos(\pi f_0/f_s) \sin(\pi N f/f_s) \sin(\pi f/f_s)}{\cos(2\pi f/f_s) - \cos(2\pi f_0/f_s)} \quad (16)$$

Compensation for the filter gains may be achieved through the use of eqns. 15 and 16. However, since the correct frequency cannot be determined without correct compensation, it is necessary to incorporate the compensation process in a feedback loop.

The second cause of error is due to the assumption to piecewise linearity between sample intervals when making the derivative calculation. It is shown in Appendix 7.2, that the right hand side of eqn. 14 equates, not simply to f, but to the term $f - 2\pi^2 f^3 \Delta T^2/3$. For a practical implementation of the frequency measurement algorithm using a microprocessor, the computation required to solve this term for f is not justified. Instead, accuracy can be improved by, firstly, evaluating the following expression:

$$f_{err} = \frac{2\pi^2 f^3 \Delta T^2}{3} \quad (17)$$

and, secondly, adding f_{err} to the current frequency estimate, that is, the measured frequency becomes $f + f_{err}$. Numerical examples of this approach, assuming a sampling frequency of 4 kHz, are shown in Table 1. This Table shows that the approach correctly evaluates the power system frequency to within three places of decimals.

Table 1: Effect of derivative error and associated compensation technique on calculation of power system frequency (for f_s = 4 kHz)

Power system frequency, Hz	f (from eqn. 14)	f_{err} (from eqn. 17)	$f + f_{err}$
48.0	47.954 52	0.045 35	47.999 87
50.0	49.948 60	0.051 25	49.999 85
52.0	51.942 18	0.057 63	51.999 81

2.4 Frequency calculation algorithm

Taking into account the factors described in the preceding sub-Sections, a new algorithm for the calculation of power system frequency is proposed. The overall structure of the algorithm is shown in Fig. 2.

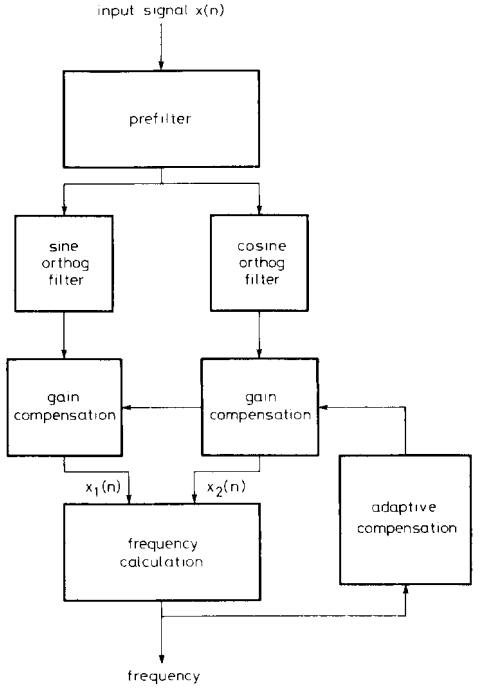

Fig. 2 *Structure of the frequency measurement algorithm*

The input to the algorithm is a sequence of discrete time values of the power system signal; it is assumed that the values have been sampled correctly and no aliasing has occurred. The prefilter is required to filter out any components contained within the sampled input signal which will not be removed by the FIR sine and cosine orthogonal filters. This is of particular relevance to power system frequency harmonics. Although the FIR filters show complete rejection of harmonics when the power system frequency is 50 Hz (Fig. 1*a*), this is not the case for other values of power system frequency. For example, if the frequency is 47 Hz, then the third harmonic frequency will consequently be 141 Hz which, from Fig. 1*a*, will not be rejected by the orthogonal filters. Thus, to ensure high accuracy under all conditions, it is necessary to include a prefilter to ensure that only signals at power system frequency are processed by the algorithm. Investigations showed that a FIR Hamming type filter with a filter length at least equal to the period of the lowest encountered power system frequency provided good rejection of likely harmonics yet retained high speed measurement of frequency.

The sine and cosine orthogonal filter blocks in Fig. 2 correspond to the implementation of the FIR filters described by eqns. 10 and 11; the coefficients of these filters are precalculated. The frequency calculation is the implementation of eqn. 14 together with the compensation for the derivative error given by eqn. 17. In order to compensate for the gains of the orthogonal filters at the most recent measurement of frequency, a feedback process is incorporated in the algorithm. However, care must be taken at this stage to ensure that the algorithm remains stable to changes in frequency and, more importantly, changes in signal amplitude. The block marked adaptive compensation performs the gain compensation by calculating the best estimate of the frequency from the previous 5 ms ($\frac{1}{4}$ cycle) history of the frequency and amplitude of the input signal. Justification for this step is given in Appendix 7.3. Having calculated the filter gains, the outputs of the orthogonal filters are multiplied by the reciprocal of the relevant gain to ensure that the magnitudes are equal.

3 Performance evaluation

Computer simulation results are presented for the frequency measuring algorithm to show its performance under steady-state conditions, dynamic conditions, and to signals containing harmonic content. The algorithm was simulated with a sampling frequency of 4 kHz and included a 100 coefficient Hamming type prefilter.

Figs. 3*a* and *b* show the response of the algorithm to steady state sinusoids at 52, 50 and 48 Hz, respectively. The accuracy of the algorithm is seen from these results to be within 0.001 Hz as predicted in Section 2.3. For all results in this section, the operation of a 16 bit analogue to digital converter was included to simulate the effects of quantisation. The accuracy of the frequency measurement was consistent for all amplitudes of the unquantised input signal in the range 1.0 to 0.05 p.u. An important feature of the algorithm is that a new measurement of frequency is made during every sampling interval, i.e., 4000 measurements are made every second. Frequency measurement is made irrespective of the phase of the input signal.

Dynamic conditions were investigated by using the 'electromagnetics transient program' (EMTP) to simulate the simple system of Fig. 4*a* which shows a 75 MVA generator connected to, initially, a load of 36.2 MW. Parameters used in this simulation are shown in Appendix 7.4. At time $t = 15.205$ s the switch is closed, thus loading the generator with an additional 17.8 MW. In this simulation, the operation of the speeder motor in the governor is disabled and hence the new loading condition results in a new steady state system frequency below the

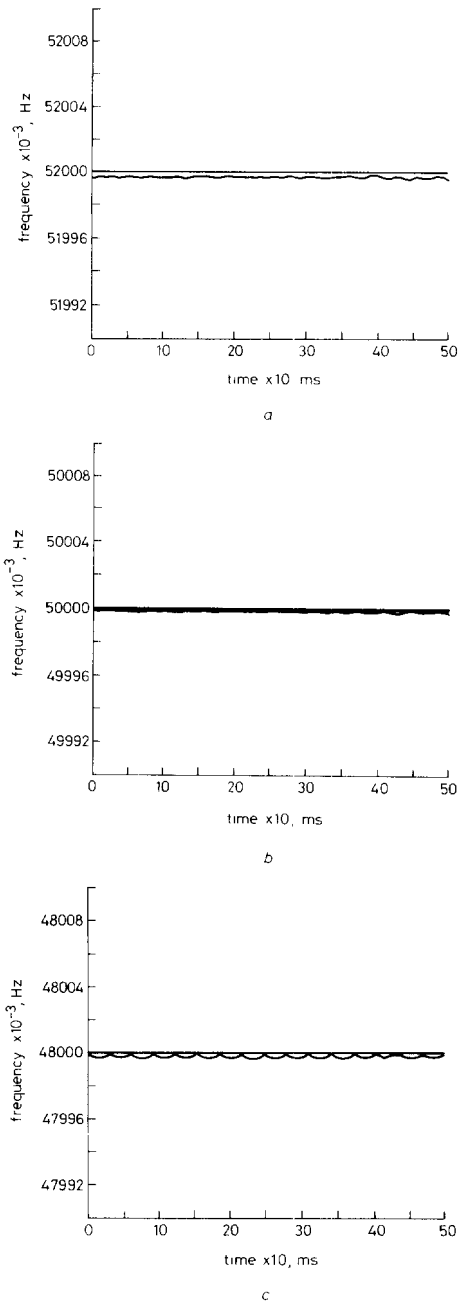

Fig. 3 *Response of algorithm to steady-state sinusoid*
a At 52 Hz
b At 50 Hz
c At 48 Hz

nominal. Fig. 4*b* shows the generator terminal voltage which is both frequency and amplitude modulated. This voltage was processed by the algorithm and the resulting frequency is depicted in Fig. 4*c* together with the generator rotor speed obtained from the EMTP simulation.

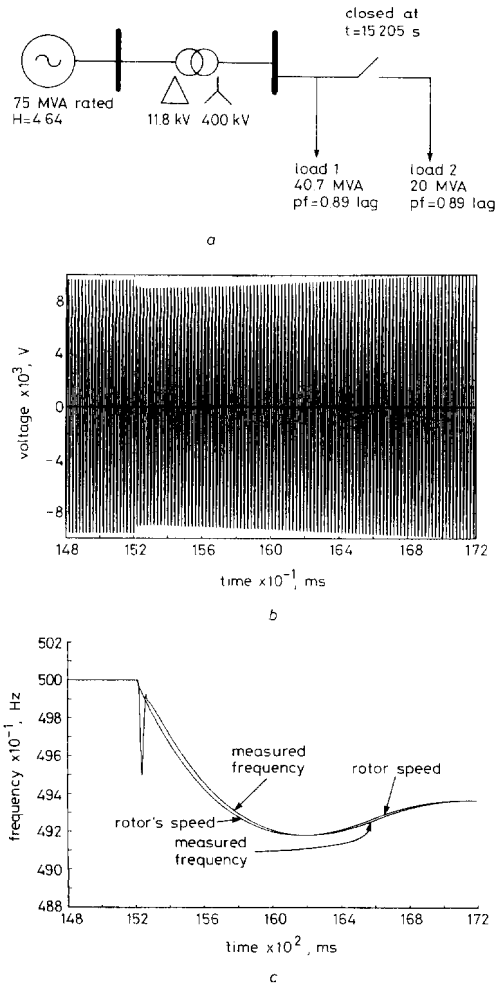

Fig. 4 *Algorithm performance for single machine power system*
a Simple single machine power system
b Generator terminal voltage
c Measured frequency and rotor speed

When the switch is closed, an instantaneous change in the terminal voltage occurs due to the redistribution of power. This is responsible for the initial 0.5 Hz 'spike' in the algorithm output at 15.2 s and is a consequence of measuring frequency from the terminal voltage. There is, of course, no corresponding instantaneous change in the rotor position and so the rotor speed is not seen to vary in the same way. Ignoring this effect, it can be clearly seen from Fig. 4*c* that the algorithm closely follows the rotor speed and exhibits a constant delay in frequency measurement of approximately 25 ms. Both rotor speed and algorithm output settle to a constant frequency of 49.37 Hz at approximately 2 s after the initial overload.

Fig. 5 shows a more complicated power system section with two generators connected to a common busbar via transmission line sections. Parameters used in this simulation may be found in Appendix 7.5. Initially, the generators at P and Q are loaded to 831.2 MW whereas the infinite bus infeed is 249.4 MW. At time $t = 15.015$ s the connection to the infinite bus is removed, the system becomes isolated, and thus the two generators take up the total load. Fig. 6 shows the frequency measured from

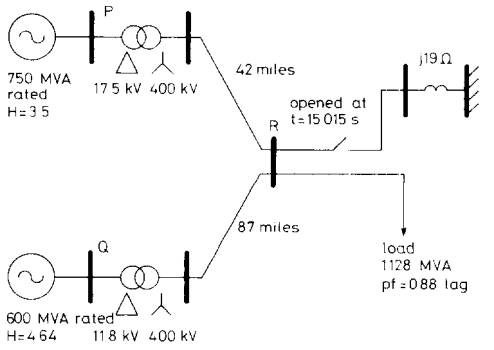

Fig. 5 *Two machine system with infinite bus connection*

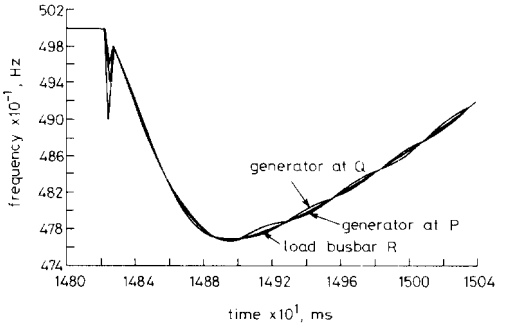

Fig. 6 *Frequencies evaluated from voltages measured at generator terminals and busbar R*

voltages taken from the terminals of the two generators, i.e., busbars P, Q and the load busbar R. For clarity, the EMTP output frequencies apparent at these positions are not shown in Fig. 6. However, as with the previous results, the algorithm exhibited perfect tracking of the frequencies with a 25 ms delay. The algorithm clearly shows the frequency oscillations resulting from power swings between the two generators in the isolated power island; the load bus frequency is observed to be approximately the mean of the two generator frequencies. These results show that the algorithm can track relatively fast frequency variations.

Finally, Fig. 7 shows the response of the algorithm to a dynamically changing power system signal having 10% of third harmonic and 5% of fifth harmonic. The signal has constant fundamental and harmonic amplitudes but exponentially decaying frequency. This is a particularly severe test because, due to the change in the power system frequency from 50 to 41 Hz, the third and fifth harmonic will vary from 150–123 Hz and 250–205 Hz, respectively. It is the action of the Hamming prefilter which ensures correct frequency measurement for this case; examination of Fig. 7 will reveal no discernable effect from the harmonics.

4 Algorithm structure for multiple input signals

The input signal to the algorithm can be either a voltage or current signal, although, in most practical cases, the input is likely to be a voltage signal. In the event that the single input signal to the algorithm is lost, either due to a fault on the chosen phase, or due to voltage transformer failure, then the frequency output of the algorithm will be similarly lost. To safeguard against this occurrence in situations where the measurement of frequency by the algorithm is critical to the correct operation of the power system, a structure for the algorithm has been developed where all three phases voltages are used. This is shown in Fig. 8 where the orthogonalisation of the three inputs signals is used to form a positive phase sequence component of the input voltage. The frequency is consequently calculated from this pps signal. The results of using this structure do not significantly vary from those shown in the previous section except that the algorithm still gives correct operation even if one of the input signals is removed. In general, under fault conditions, pps quantities are always present and so the correct measurement of frequency is ensured under even the most onerous conditions.

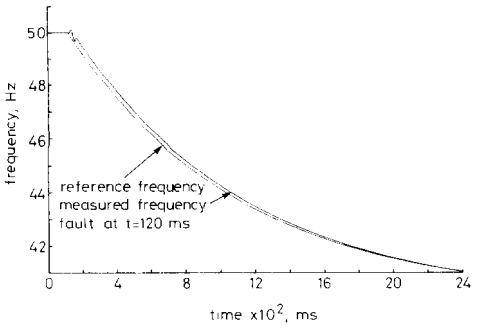

Fig. 7 *Response of algorithm to signal with exponentially decaying fundamental frequency plus 10% 3rd and 5% 5th harmonically related components*

5 Conclusions

A frequency measurement algorithm capable of evaluating power system frequency from discrete time signals has been shown to be accurate to within 0.001 Hz. The algorithm calculates a new estimate of frequency at every sampling interval irrespective of the phase of the input signal. The algorithm is capable of accurately tracking frequency under dynamic power systems conditions and provides high-speed measurement, exhibiting a delay of only 25 ms. The algorithm has shown immunity to the presence of harmonics and can be based on a three signal input with positive phase sequence component evaluation to provide a highly reliable frequency measuring function.

An important benefit of the algorithm is that it calculates frequency through a wholly numeric process and is based upon discrete time signals captured at a fixed sampling rate. It is thus suitable for implementation in current numeric protection relay hardware. The algorithm will find applications where high-speed frequency measurement is critical such as in under frequency relays and load shedding schemes.

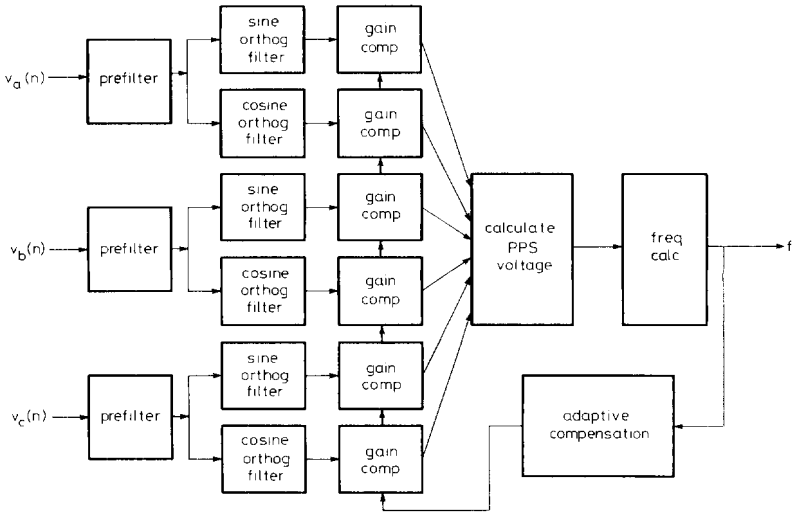

Fig. 8 *Structure of frequency measurement algorithm capable of deriving positive phase sequence component of three phase input signals*

Currently, work is progressing on the implementation of the algorithm on hardware incorporating a digital signal processor. It is hoped to report on this development in due course.

6 References

1 GIRGIS, A.A., and HAM, F.M.: 'A new FFT-based digital frequency relay for load shedding', *IEEE Trans. Power Appar. & Syst'*. Feb. 1982, **PAS-101**, (2), pp. 433–439

2 PHADKE, A.D., THORP, J.S., and ADAMIAK, M.G.: 'A new measurement technique for tracking voltage phasors, local system frequency and rate of change of frequency', *IEEE Trans. Power Appar. & Syst.*, May 1983, **PAS-102**, (5), pp. 1025–1038

3 MALIK, O.P., HOPE, G.S., HANCOCK, G.C., ZHAOHUI, L., LUQING, Y., and SHOUPING, W.: Frequency measurement for use with a microprocessor-based turbine governor'. Paper No. 91 WM 140-4EC, IEEE PES Winter meeting, New York, Feb. 1991

4 McILWAINE, S.A., TINDALL, C.E., and McCLAY, W.: 'Frequency tracking for power system control', *Proc. IEE, C.*, March 1986, **133**, (2), pp. 95–98

5 BENMOUYAL, G.: 'Design of a combined global differential and volt/hertz relay for step-up transformers', *IEEE Trans. Power Delivery*, July 1991, **6**, (3), pp. 1000–1007
6 GIRAY, M.M., and SACHDEV, M.S.: 'Off nominal frequency measurements in electric power systems', *IEEE Trans. Power Delivery*, July 1989, **4**, (3), pp. 1573–1578
7 GIRGIS, A.A., and HWANG, D.: 'Optimal estimation of voltage phasors and frequency deviations using linear and nonlinear Kalman filtering: theory and limitations', *IEEE Trans. Power Appar. & Syst.*, Oct. 1984, **PAS-103,** (10), pp. 2943–2949
8 SACHDEV, M.S., WOOD, H.C., and JOHNSON, N.: 'Kalman filtering applied to power systems measurements for relaying', *IEEE Trans. Power Appar. & Syst.*, Dec. 1985, **PAS-104,** (2), pp. 3565–3573
9 GIRGIS, A.A., and PETERSON, L.W.: 'Adaptive estimation of power system frequency deviation and its rate of deviation for calculating sudden power system overloads', *IEEE Trans. Power Delivery*, Apr. 1990, **3**, (2), pp. 585–594
10 KAMWA, I., and GRONDIN, R.: 'Fast adaptive schemes for tracking voltage phasor and local frequency in power transmission and distribution systems', *IEEE Trans. Power Delivery*, Apr. 1992, **7**, (2), pp. 789–795
11 PAPOULIS, A.: 'Random modulation: a review', *IEEE Trans. Acoust., Speech & Signal Process.*, Feb. 1983, **ASSP-31,** (1), pp. 96–105
12 MASON, T.H., AYLETT, P.D., and BIRCH, F.H.: 'Turbogenerator performance under exceptional operating conditions', *IEE Proc. A*, Jan. 1959, paper 2846-S, pp. 357–373

7 Appendices

7.1 Magnitude gains of the sine and cosine filters

The FIR expression for the sine filter is given by

$$H_s(k) = \sin\left(\frac{2\pi K}{N} + \frac{\pi}{N}\right) \quad \text{for } k = 0, 1, \ldots, N-1 \tag{18}$$

which is the product of a sinusoidal function and a rectangular window $p(k)$, where $p(k) = 1$ for $k = 0, 1, 2, \ldots, N-1$ and $p(k) = 0$ otherwise. An expansion of eqn. 18 will yield:

$$H_s(k) = p(k)\sin\left(\frac{2\pi k}{N}\right)\cos\left(\frac{\pi}{N}\right) + p(k)\cos\left(\frac{2\pi k}{N}\right)\sin\left(\frac{\pi}{N}\right) \tag{19}$$

In the frequency domain, the Z transform of eqn. 19 is

$$H_s(z) = \tfrac{1}{2}\sin\left(\frac{\pi}{N}\right)[P(ze^{j\Omega_0}) - P(ze^{-j\Omega_0})] + j\tfrac{1}{2}\cos\left(\frac{\pi}{N}\right)[P(ze^{j\Omega_0}) + P(ze^{-j\Omega_0})] \tag{20}$$

where

$$P(z) = \frac{z - z^{-(N-1)}}{z+1}, \quad \Omega_0 = \frac{2\pi f_0}{f_s} \tag{21}$$

which includes f_0, the frequency of sinusoid of eqn. 18, and f_s is the sampling frequency.

Solving for $P(z)$, the Z transform of eqn. 18 becomes

$$H_s(z) = \frac{\sin\left(\frac{\Omega_0}{2}\right)(1 - z^{-N})(z+1)}{z - 2\cos\Omega_0 + z^{-1}} \tag{22}$$

Since the filters are causal, the one-sided Z transform may be used where $z = re^{j\Omega}$ for $r = 1$, i.e., lying on the unit circle in the Z plane. From eqn. 22,

$$H_s(e^{j\Omega}) = \frac{j2e^{-j\Omega(N-1)/2}\sin(\Omega_0/2)\sin(N\Omega/2)\cos(\Omega/2)}{\cos\Omega - \cos\Omega_0} \tag{23}$$

By a similar procedure, the frequency domain expression of the cosine filter may be derived,

$$H_c(e^{j\Omega}) = \frac{-2e^{-j\Omega(N-1)/2}\cos(\Omega_0/2)\sin(N\Omega/2)\sin(\Omega/2)}{\cos\Omega - \cos\Omega_0} \tag{24}$$

Eqns. 23 and 24 can be expressed in terms of their magnitude and phase response for $\Omega = 2\pi f/f_s$,

$$|H_s(f)| = \frac{2\sin(\pi f_0/f_s)\sin(\pi N f/f_s)\cos(\pi f/f_s)}{\cos(2\pi f/f_s) - \cos(2\pi f_0/f_s)} \tag{25}$$

and

$$\angle H_s(f) = je^{-j\pi f(N-1)/f_s} \tag{26}$$

Similarly for the cosine filter,

$$|H_c(f)| = \frac{2\cos(\pi f_0/f_s)\sin(\pi N f/f_s)\sin(\pi f/f_s)}{\cos(2\pi f/f_s) - \cos(2\pi f_0/f_s)} \tag{27}$$

and

$$\angle H_c(f) = -e^{-j\pi f(N-1)/f_s} \tag{28}$$

7.2 Frequency error due to numerical derivative calculation

The assumption of piecewise linearity between samples, and the subsequent derivative calculation using eqn. 12, causes a time invariant frequency error to occur. This error may be conveniently derived with reference to two, unity amplitude, orthogonalised signals:

$$x_1(t) = \sin(\omega t + \phi) \quad x_2(t) = \cos(\omega t + \phi) \tag{29}$$

Thus, applying eqn. 12 to $x_1(t)$ gives

$$x_1'(t) = \frac{\sin(\omega t + \phi) - \sin(\omega(t - \Delta T) + \phi)}{\Delta T} \tag{30}$$

which may be re-expressed as

$$x_1'(t) = \frac{\sin(\omega t + \phi) - (\sin(\omega t + \phi)\cos(\omega\Delta T) - \cos(\omega t + \phi)\sin(\omega\Delta T))}{\Delta T} \tag{31}$$

Replacing $\cos(\omega\Delta T)$ and $\sin(\omega\Delta T)$ with the first two terms of the relevant Maclaurin series, eqn. 31 may be written as

$$x_1'(t) = \frac{\sin(\omega t + \phi) - \left[\sin(\omega t + \phi)\left(1 - \frac{(\omega\Delta T)^2}{2!}\right) - \cos(\omega t + \phi)\left(\omega\Delta T - \frac{(\omega\Delta T)^3}{3!}\right)\right]}{\Delta T} \tag{32}$$

which simplifies to

$$x_1'(t) = \omega\cos(\omega t + \phi) + \sin(\omega t + \phi)\frac{\omega^2\Delta T}{2} - \cos(\omega t + \phi)\frac{\omega^3\Delta T^2}{6} \tag{33}$$

An expression for $x_2'(t)$ may be similarly derived:

$$x_2'(t) = -\omega\sin(\omega t + \phi) + \cos(\omega t + \phi)\frac{\omega^2\Delta T}{2} + \sin(\omega t + \phi)\frac{\omega^3\Delta T^2}{6} \tag{34}$$

The analytic expressions for $x'_1(t)$ and $x'_2(t)$ may now be substituted into the frequency evaluation expression, eqn. 5, to yield the following result:

$$x_2(t)x'_1(t) - x_1(t)x'_2(t) = \omega - \frac{\omega^3 \Delta T^2}{6} = 2\pi\left(f - \frac{2\pi^2 f^3 \Delta T^2}{3}\right) \quad (35)$$

Thus it will be apparent from eqn. 35 that the numerical derivative calculation introduces a nonlinear error in the frequency evaluation process.

7.3 Adaptive compensation

The input signal to the frequency measurement algorithm may be considered to be both frequency modulated and amplitude modulated, in either case the modulation is taken to be random. It has been shown [11] that the optimum estimation of the frequency, $f^*(t)$, of a signal having a randomly varying amplitude $X(t)$ is given by

$$f^*(t) = \frac{E[X^2(t)f(t)]}{E[X^2(t)]} \quad (36)$$

where $E[\cdot]$ denotes the expected, or mean, value of the variable in parenthesis. In the frequency measurement algorithm, the expected value can be approximated by a moving average filter, for example, the expected value of some discrete time variable $x(n)$ can be calculated from its previous time history:

$$E[x(n)] \approx \frac{\sum_{i=0}^{N-1} x(n-i)}{N} \quad (37)$$

Thus eqn. 37 is applied individually to the square of the amplitude, $X(t)$, of the input signal (given by eqn. 6) and to the product of the amplitude squared and the frequency estimate from the algorithm output. The quotient of these terms, i.e., eqn. 36, is then used to calculate the filter gains from eqns. 15 and 16. A series of tests showed that moving average filter lengths of 5 ms (i.e., $N = 20$ for $f_0 = 50$ Hz and $f_s = 4$ kHz) promoted the best algorithmic response to typical dynamic power system input signals.

7.4 Parameters used to model single machine system (Fig. 4a)

Units in ohms unless otherwise stated.

Transformer:	leakage reactance (LV side) = 0.0435 leakage reactance (HV side) = 37.51
Generator:	75 MVA rated, 50 Hz, 2 pole, 11.8 kV, $H = 4.64$ s $x_d = 2.0$, $x_q = 1.9$, $x'_d = 0.2$, $x'_q = 0.19$. For further details, see Reference 12.

7.5 Parameters used to model two machine system (Fig. 5a)

Units in ohms unless otherwise stated.

Transmission lines:	modelled as pi equivalents, = circuit parameters per mile: $R = 0.039$, $L = 62.4$ mH, $C = 20.3$ nF.
Transformer at P:	leakage reactance (LV side) = 0.0833 leakage reactance (HV side) = 26.03
Transformer at Q:	leakage reactance (LV side) = 0.0435 leakage reactance (HV side) = 37.51
Generator at P:	750 MVA rated, 50 Hz, 2 pole, 17.5 kV, $H = 3.5$ s $x_d = 1.75$, $x_q = 1.75$, $x'_d = 0.265$, $x'_q = 0.265$
Generator at Q:	modelled as eight parallel 75 MVA units as described in Fig. 4a. For further details, see Reference 12.